Neutral-Current Detection in SNO – A Position Paper

R. G. H. Robertson

June 6, 1991
SNO-STR-91-026

Abstract

Strategies for the detection of neutrons in the SNO heavy water have been considered from the standpoints of physics capability, signal, background sources, background magnitudes, background measurement, systematic effects, engineering complexity, and coexistence between different strategies. Consideration of costs is deferred. It is recommended that, by the time SNO is commissioned, it should be capable of accommodating a) the "White Book" option (NaCl dissolved in the total volume of heavy water, b) a split vessel option (a median-plane membrane dividing the vessel into salted and pure heavy water), and, c) discrete detectors containing helium-3.

1 Introduction

This position paper is a draft for discussion and a framework for a final Neutral Current Design Criteria Document.

2 Physics Objectives

In order of priority, the neutron-detection capability must allow:

1. A measurement of the total flux of left-handed neutrinos emitted by the sun, averaged over a period of one year.

2. A measurement of the total flux of left-handed neutrinos emitted by the sun, averaged over a period of one month.

3. A measurement of the instantaneous total flux of left-handed neutrinos emitted by the sun or by a supernova, distinguished event-by-event from other types of interactions.

3 Methods

The following methods are presently under consideration to meet one or more of the physics objectives.

1. Salt dissolved in the D_2O (White Book method).
2. Scintillator/wls and salt in the D_2O – NC events group in a sharper peak for quasi-real-time stripping.
3. Split vessel. Upper/lower hemispheres containing salt/nothing or some other combination.
4. Split vessel. Inner/outer spheres with a bladder to separate the volumes. Inner/outer are doped with salt/something else.
5. Proportional counters with ^3He.
6. Scintillators with ^3He. Readout via existing PMT array or optical fibers.
7. Lithium-6 sheets with scintillator or proportional-counter readout of alpha-triton pairs. In addition, the following methods have previously been considered and rejected:

8. Dissolved Gd in the heavy water. It was hoped that the gamma multiplicity in neutron capture would allow an event-by-event discrimination of NC and CC events. The isotropy was insufficient for good discrimination and the total light output was too low for good efficiency.

9. Doping the acrylic vessel walls with Gd and a scintillator. Neutron captures occur at a location where the background is high, and the method is inflexible.

10. Solid or liquid scintillators in the vessel. The pulse-height defect places neutron captures in a spectral region of high electron and gamma background. Purity requirements are too intimidating.

11. Solid scintillator beads in suspension in the heavy water. This avoids the pulse-height defect problem (the beads are too small for appreciable electron energy loss), but the U purity requirements (6×10^{-14} ng/g) and considerable scattering of Čerenkov light make the method unattractive [12].

12. NaCl in tubes. Encapsulating the salt simplifies the water treatment system enormously, but makes it inaccessible to the radon-assay background measurement technique that is the major reason for dissolving salt in the heavy water directly. The net efficiency is low (about 25%).

4 Acceptance Criteria

The method(s) selected must satisfy the basic criterion that the conclusions drawn by SNO concerning the flux of left-handed neutrinos be non-trivial and unassailable.

This basic criterion can be decomposed into more specific criteria:

1. Unambiguous identification of neutron signal.
2. Adequate statistical accuracy
3. Independent measurements of or limits on all known backgrounds.
4. Contemporaneous measurement of backgrounds
5. Confirmation of result by a separate method with different systematics.

There are further criteria that safeguard the physics productivity of SNO:

1. Acceptable interference with charged-current and elastic-scattering signals.
2. Good duty factor.
3. Stable, low-maintenance operation.

In addition there are criteria related to practicality:

1. No significant personnel hazard
2. No significant risk to heavy water
3. Achievable engineering
4. Realistic cost.

5 The Decision Process

The following factors influence the nature and timing of our decisions: Decisions should be delayed as long as possible because:

1. The quantity and quality of the input information is maximized
2. The risk of choosing a method that later proves unworkable is minimized.
3. Flexibility in adding or deleting methods is maximized.

Decisions should be made as promptly as possible because:

1. Manpower and costs being devoted to eliminated methods can be freed up for other uses.

2. Funding agencies have deadlines that lead the fiscal year by up to 2 years. Proposals require additional time beyond that to prepare.

3. Methods have interfaces with other parts of SNO (acrylic vessel, H_2O, D_2O, mechanical, etc.) that have imminent deadlines.

4. Methods require long-term testing and verification before deployment.

From these countervailing factors and the acceptance criteria emerges one consistent plan:

By the time SNO is commissioned, it must be capable of supporting at least two methods of neutral-current readout. There is no incentive to support more than 3 methods. The methods selected must be chosen to be compatible with each other, and to constrain the design of SNO to the minimum extent possible. Work on methods not selected should be discontinued in favor of more urgent needs in SNO. Methods selected, however, should be designed with a careful eye on the possible need to reactivate a non-selected method as R&D progresses.

6 Neutral Current Signal

The possible neutral-current rate ranges from the standard solar model (SSM) rate to about 1/3 SSM rate. What *is* the SSM rate per kilotonne-year?

White Book [10]	6380
Bahcall et al. [8]	4500
Ying et al. [9]	4900

The White Book value was chosen as the largest in the literature. The Ying et al. calculation is probably the best, because it is the only one to include forbidden contributions to the interaction cross section.

The spectrum of CC events can be distorted by MSW-enhanced oscillations or neutrino magnetic moments. The NC spectrum may or may not be distorted, depending on physics (MSW and sterile or right-handed neutrinos). However, even if it is distorted, we are assured that the rate cannot be less than about 1/3 SSM because CC events have already been observed at that level with energies above 8 MeV, where the cross section is largest.

The most difficult case would be a number around 1/3 SSM. For comparison of methods, the actual rate is not crucial, and we adopt a neutron production rate of 5000 per kt-y.

7 Reference Designs

7.1 White Book (revised)

- 1000 tonnes of heavy water.
- 2.5 tonnes of NaCl
- 56% coverage at 18% anode efficiency.

	U	Th	
D_2O	0.011	0.011	pg/g
H_2O	0.015	0.022	pg/g
NaCl	1.0	1.0	pg/g
Acrylic	3.6	1.9	pg/g

7.2 Scintillator/Wavelength Shifter

Scintillator : No reference design owing to lack of data.

Wavelength shifter:

- Čerenkov component in visible unaffected.
- Added isotropic component equal to 2 times N_{hit}.
- Negligible radioactivity.

7.3 Split Vessel

- Median-plane split of 0.25-mm Teflon.
- Upper half pure D_2O
- Lower half with 1.25 tonnes of NaCl.

	U	Th	
Teflon	12	12	pg/g
NaCl	1	1	pg/g

7.4 Bladder

- Spherical bladder concentric with acrylic vessel
- 0.25-mm Teflon
- Radius 4.76 m
- 1.25 tonnes NaCl inside
- 1.25 tonnes of neutron-absorbing salts outside.

	U	Th	
Teflon	12	12	pg/g
NaCl	1	1	pg/g
Salts	1	1	pg/g

7.5 Helium-3 Proportional Counters

- 109 strings on 100-cm square lattice
- Total length of detectors 900 m
- Acrylic bodies 2.54-cm outer radius, 3-mm wall
- 3 atm helium-3
- 0.3 atm xenon

- Anode wire 0.025-mm diameter copper
- Cathode 0.025-mm copper film
- End-caps acrylic (900 x 50 g) plus glass (900 x 10 g)
- Fill tubes copper (450 x 1.5 g)

	U	Th	
Acrylic	3.6	1.9	pg/g
Copper	2.0	2.0	pg/g
Glass	20	20	pg/g

7.6 Helium-3 Scintillators

- 109 strings on 100-cm square lattice
- Total length of detectors 900 m
- Suprasil T-21 silica bodies 2.5-cm outer radius, 2-mm wall
- 3 atm helium-3
- 0.3 atm xenon

	U	Th	
Silica	3.2	6.8	pg/g

7.7 Lithium-6 Proportional Counters or Scintillators

- 330 strings on 60-cm square lattice
- Total length of detectors 3000 m
- Acrylic bodies 1.8-cm radius, 3-mm wall
- 3 layers of ^{6}Li, 95% enriched, each 10 μm thick, 2 cm wide
- Supported on 0.5-μm stretched polypropylene
- 10 atm xenon

8 Čerenkov Options

The NC and CC events are both converted to Čerenkov light and cannot be distinguished on an event-by-event basis. The shape of the NC spectrum can be determined by calculation and calibration. The CC spectrum is not known *a priori*. The NC and CC spectra are therefore separated by subtraction. In principle, the two can be separated by fitting, but Frati and Beier [1] have shown that, even if both spectral shapes were known, this procedure is extremely sensitive to calibration errors, and therefore unreliable.

8.1 White Book (Revised)

In the revised White Book (WB) option, the experiment runs alternately with salt in and out. The procedure has been revised to allow for salt addition and removal underground to address the requirement of contemporaneous background measurement. It is estimated that the transition from salt in to less than 50 ppm salt will take about 25 days, which dictates a minimum cycle time of order 2 months or greater. Over a period of a year, then, the statistical powers of the WB and split-vessel options are comparable. However, the split-vessel options are always prepared for a transient event such as a supernova, whereas the WB option has only a 50% chance of being in the fully NC-sensitive mode (there is always a little sensitivity from neutron capture on deuterium, and elastic scattering).

Backgrounds arise from any process that creates neutrons in the heavy water, but the only significant one is photodisintegration of deuterium by the 2.6- and 2.44-MeV gammas at the bottom of the Th and U decay chains. Cosmic-ray, fission, (α,n) and external neutrons are negligible. The activities of the U and Th chains below Ra are relevant, and will be determined by adsorbing the 3.6-day ^{224}Ra and 1602-yr ^{226}Ra on MnO_2-coated fibers or in crown-ether compounds, and counting the daughter Rn activities in a time projection chamber.

Recently it has been noted that an error in this procedure would be made if significant amounts of 56-s ^{220}Rn or 3.8-day ^{222}Rn emanated from the acrylic vessel into the heavy water. The former is the more worrisome, because 10.6-hr ^{212}Pb can migrate some distance into the vessel before decaying to give, ultimately, a 2.6-MeV photon. There is a reasonable prospect of detecting the longer-lived radon directly from the heavy water if it were present.

An independent means for determining the 2.6- and 2.44-MeV photon flux in the heavy water is therefore desirable, and efforts to recover this information from the background "wall" are in order. In combination with the radium extraction, it may then be possible to unravel the U and Th contributions separately. It is important to establish whether there will be contributions to the wall that are unrelated to high-energy gammas.

For the present purposes, we assume that the White Book operating mode will be to run with salt in and out for equal periods of time and subtract the two spectra to obtain a net neutron-capture spectrum. We neglect the confounding effect of the transition time during which there is an intermediate concentration of salt – with the proper analysis this will make a negligible contribution to the total uncertainty because it delivers good data with a different proportion of neutron signal. This mode of analysis is independent of knowledge of the shapes of spectra or of Monte Carlo results, but it requires that there be no (unknown) time-dependence in the data or the background. If the neutron-capture spectrum shape is known from calibrations, then each point in the subtracted spectrum is an independent determination of the neutron flux, and the net uncertainty is obtained from the usual weighted average. Figures 1-4 show the raw and subtracted spectra for the SSM and SSM/3 fluxes. The internal background has not been subtracted.

We calculate for the White Book option, and every other option, the uncertainty in the total neutron production rate. We also calculate the uncertainty in the net NC rate subject to the assumption that U and Th in the D_2O produce 1176 neutrons per kt-y. When NaCl is present as well at 0.25% concentration, an additional 294 neutrons per kt-y are produced. It is assumed that the total background neutron rate from these sources can be determined by radon-assay and by Cerenkov counting of the beta-gamma background to an accuracy of 20%. The calculation is done for NC rates of 5000 per kt-y, and 5000/3 per kt-y.

NC neutrons	5000	1667
Internal neutrons	1470	1470
Total neutrons	6470	3137
σ_t	186	147
σ_{int}	294	294
σ_t/t	2.9%	4.7%
σ_{NC}/NC	7.0%	19.7%

The dominant role of the 20% uncertainty in the background determination is obvious.

8.2 Scintillator/Wavelength Shifter

The desirability of extracting useful information from the background wall was the initial motivation for considering the addition of scintillator/wls to the heavy water [5]. Subsequently it was realized that lower thresholds and a narrower NC peak might also result.

The width of the NC distribution in the standard WB option is determined by the fluctuations in shower formation and by photon statistics. Frati and Beier show that the distribution is Gaussian with a centroid at 59 hits and a standard deviation of 15. If photon statistics alone were the dominant factor, the standard deviation would be 7.8 hits. Therefore the fluctuation contribution is 12.9 hits.

A wavelength shifter (wls) converts hard UV photons that would otherwise not be detected into visible photons. The Cerenkov threshold is still enforced. Hargrove and Willis added p-methyl-umbelliferone to D_2O in a neutrino experiment (E31) at LAMPF and obtained a factor of 3 increase in the light output. It is hard to conceive of doing better, because the available extra light can only come from a band between about 200 and 350 nm. It is bounded on the short-wavelength side by absorption in the water itself, and on the long-wavelength side by the fact that such photons are already being detected. If this factor of 3 were to be achieved in SNO, then the photon statistics component would fall to 4.5 hits, and the total NC distribution width would decrease from 15 to 13.7 hits standard deviation. This improvement in width is negligible and would offer no qualitative gain in the extraction of the NC signal from the data.

The conversion of the heavy water into a scintillation medium offers potentially significant gains in resolution through reduction of both the photon-statistics and fluctuation components. It is not possible to be quantitative about it in the absence of detailed information. However, there are formidable practical objections to both scintillators and wls:

1. Is there an additive in existence that is known to work well enough to meet our physics requirements? Would we have to sacrifice directional information?
2. How would the additive affect the water-purification strategy?
3. How would the additive affect the method for assaying U and Th?
4. Would there be a hazard presented to the acrylic?
5. How would the clean-up of heavy water at the end be affected?
6. Would scattering and absorption of light affect reconstruction adversely?
7. It appears likely that, to make water scintillate, at least a fraction of a percent of additive would be needed (several tonnes). How much would exchange of protons for deuterons downgrade the heavy water?
8. Loss of the Cerenkov threshold exposes us to high or unknown rates from low-energy beta and gamma emitters. The immediate concern is allowable tritium levels and effective PMT "dark" rates. (The specified maximum tritium level of 0.05 microCurie/l and a photon yield 10 times higher than Cerenkov light alone gives a rate of 20 kHz per tube, to be compared with the specified dark rate of 6 kHz. Bearing in mind that the number of hits is increased 10-fold, this does not appear to be a fatal difficulty.)

On the other side of the issue is the chance that SNO might be able to operate with a much lower threshold. More of the CC distribution might be visible, and perhaps CNO, pep and ^{7}Be neutrinos might even be observable. Determination of the crucial 2.62- and 2.44-MeV gamma rates might be easier. These things are tempting, but very uncertain.

We conclude that the addition of a wls offers no advantages for NC signal recovery *per se*. A scintillator might be of value, but is not required for the NC program. Development of such a material is an R&D program that may well be beyond the capabilities of the existing collaboration, and could undermine our ability to meet the more modest goals we are committed to. Therefore neither option should be pursued specifically as a NC objective. To decide if either should be pursued for other physics is a question beyond the purview of this report.

8.3 Split Vessel Options.

The split-vessel proposal is an improvement over the WB option in that:

1. The SNO detector is always configured for NC detection.
2. The NC-CC subtraction is always made with simultaneously acquired data.
3. There is a slight statistical advantage since neutrons produced in the low-neutron absorption volume tend to migrate into salted volume where they are detected, making the effective neutron-sensitive volume greater than the geometrical share.

The drawbacks identified are:

1. Two separate water-treatment systems are needed,
2. The engineering of a split vessel is more complicated,
3. The presence of membranes within the heavy water requires a method to determine the contribution of those membranes to the backgrounds,
4. Calibration of the two separate volumes with sources that can be placed anywhere seems to be a difficult engineering problem,
5. The position of the separating membranes needs to be determined to a precision of about 10 cm over most of the surface.

Two engineering realizations of the split-vessel concept have been suggested, a median-plane split with a flexible membrane, and a spherical bladder [6] located inside the acrylic vessel and concentric with it. The median-plane split would be achieved with an "inner- tube" arrangement that was pressurized with water to seal against the wall of the acrylic vessel (a tight seal is not required). The membrane spans the hole in the doughnut. The bladder would be unfurled and located in the center of the vessel with various strings and pulleys.

The differences between the two realizations can be summarized as follows:

1. The bladder option makes use of the D_2O that is furthest from the acrylic and external gammas. If unexpectedly high backgrounds from those sources were to be present, the interspace can be filled with a neutron poison to improve the quality of the NC data in the bladder volume.

2. In the bladder geometry, the CC events are taken from the interspace, and it may appear that the higher background there makes problems for that signal, but in fact the beta-gamma threshold moves up relatively slowly with acrylic activity. The median-plane split makes two volumes that share "good" and "bad" space equally.

3. The bladder option preserves spherical symmetry for both volumes. Concerns have been expressed that the hemispherical shapes of the median-plane split will give rise to diurnal variations as CC and ES events are registered from different angles depending on the sun's position. Quantifying these concerns has proven elusive.

4. The bladder option requires the subtraction of signals obtained from different-shaped volumes. Careful calibration is therefore required in a geometry that does not lend itself easily to that. The median-plane split volumes are the same shape.

5. The bladder option uses (approximately) 4 times as much membrane area as the median-plane split.

6. The bladder requires similar densities inside and out. Therefore, whether needed for neutron absorption or not, the water treatment systems must be able to deal with two different solutes.

7. Both split-vessel options appear to be compatible with the WB and discrete-device options.

8. The engineering of the median-plane split appears to be substantially simpler than the bladder.

9. Moving calibration sources around the median-plane split volumes appears very difficult, around the bladder volumes even more difficult.

These points may be crudely summarized: If acrylic activity is the main concern, the bladder option is better. If membrane activity is the main concern, the median split vessel option is better. If neither is a concern, the median split is easier to engineer and calibrate.

Monte Carlo calculations of neutron transport in split vessels have been carried out. In Fig. 5 one sees the effect of neutron migration from the pure D_2O side across to the salted side. Twice as many captures occur on the salted side. Not surprisingly, most of these extra captures occur close to the membrane. That may increase the difficulty of disentangling membrane activity from NC events (specifically, it may increase the correlation coefficient in the fit of data to membrane plus NC rates). Figure 6 shows the distribution of events as the acrylic activity is increased.

At the measured upper limits (12 pg/g) for Teflon, the median-plane split membrane produces an additional 78 neutrons/year, and the bladder 350/year.

8.4 Čerenkov Options Compared

The methods under consideration are similar in many respects, and it is possible to find a quantitative basis for comparing them statistically. The signals that give Čerenkov light are:

1. Charged Current
2. Neutral Current (Internal + Solar)
3. ES in D_2O
4. ES in H_2O
5. Neutrons produced by acrylic radioactivity
6. Low-energy $\beta - \gamma$ backgrounds

By confining our attention to $N_{hit} > 60$ we can avoid the complications of the last item, without compromising the comparison significantly. Frati and Beier (FB) [1] carried out a detailed analysis of the White Book option, extracting each signal by parametrizing it in R^3, $\cos\theta$, and N_{hit}, and fitting data sets under various conditions. Their findings are the basis of our comparison.

In one year of running in the standard WB mode, the number of events above 60 hits are assumed to be as follows (from FB Table III):

	CC	NC	ES D_2O	ES H_2O	Acrylic
Per Year	2241(115)	2315(118)	219(29)	110(13)	234(54)

The rates are the generated ones, and the uncertainties are average values appropriate to a year's data from Maximum-Likelihood (ML) fits.

FB found that the NC and CC signals are quite similar in radial and energy dependence, and that the acrylic neutron signal was rather different, being describable by a Gaussian in R^3 (see Fig.7). This made it relatively easy to separate the acrylic and NC signals, but more difficult to separate the NC and CC signals. These facts are contained in the correlation matrix given by FB (their Table IV):

	CC	NC	ES D_2O	ES H_2O	Acrylic
CC	x	-0.71	-0.04	0.05	-0.15
NC	-0.71	x	-0.15	-0.01	-0.27
ES D_2O	-0.04	-0.15	x	-0.04	-0.02
ES H_2O	0.05	-0.01	-0.04	x	-0.14
Acrylic	-0.15	-0.27	-0.02	-0.14	x

One can see from these tables that the ES signals are not only very small, but also very weakly correlated with other signals. In other words, they decouple from the remaining 3 signals. That is not unexpected, since their angular distributions are so distinctive. To simplify the analysis, the ES signals will be neglected.

Consider a two-parameter problem in which the total number of events is sum of two separate kinds of event (e.g., NC signal and Acrylic neutrons).

$$N_t = N_N + N_A. \quad (1)$$

The variance of the total is related to the individual variances by

$$\sigma_t^2 = \sigma_N^2 + \sigma_A^2 + 2\sigma_{NA}^2, \tag{2}$$

where the covariance σ_{NA}^2 is related to the correlation coefficient by

$$\rho_{NA} = \sigma_{NA}^2/\sigma_N\sigma_A. \tag{3}$$

Therefore,

$$\sigma_t^2 = \sigma_N^2 + \sigma_A^2 + 2\rho_{NA}\sigma_N\sigma_A. \tag{4}$$

This equation defines an ellipse, the extrema of which projected on each axis give the standard deviations of each variable including correlations. At these extrema,

$$\sigma_N^2 = \sigma_A^2 = \sigma_t^2/(1 - \rho_{NA}^2). \tag{5}$$

The simplicity of this result stems from the simplicity of the problem – that the total number of events is the sum of two components. The result can be extended by induction to three or more components:

$$\sigma_i^2 = \frac{\sigma_t^2}{\prod_{i,i\neq j}(1 - \rho_{ij}^2)}. \tag{6}$$

One would expect this relationship to be generally applicable when the only statistically independent variable is the total number of counts. It is of interest to compare predictions of this analysis with the exact ML analysis of FB. We use the correlation coefficients above, neglect cross-terms, neglect the ES contributions, and compare with the two cases of WB acrylic and 10 $\times$ WB acrylic. The total numbers of events in the two cases are 4790 and 6896, respectively.

Events		4790		6896	
σ_t		69		83	
Source		Eq.(6)	FB	Eq.(6)	FB
i=CC	$\sum \rho_{ij}^2 = 0.71^2 + 0.15^2$	100	112	120	117
i=NC	$\sum \rho_{ij}^2 = 0.71^2 + 0.27^2$	106	118	127	123
i=A	$\sum \rho_{ij}^2 = 0.27^2 + 0.15^2$	72	55	87	78

The agreement is generally satisfactory, and shows the trends of the ML analysis. The worst uncertainty estimate is for the acrylic contribution at the WB level, which is only a 3% contribution to the total counts. One can, therefore, make use of the correlation coefficients and calculated numbers of events from physics to estimate uncertainties over a wide range of input conditions without repeating the complex ML analyses.

There are 4 distinct Čerenkov cases to consider, the White Book option with the NC and CC extracted by fitting (salt always present), WB with the CC measured in a salt-out run and subtracted from the salt-in data, the median-plane split vessel, and the bladder. The correlation coefficients are taken from FB. Where it is necessary to fit the activity of a membrane, it is assumed that the correlation coefficients will be identical to those for the acrylic activity. The NC-CC correlation vanishes when separate data sets are subtracted (i.e. in all cases but the first).

The total number of counts is evaluated for each case and equated to σ_t^2. The CC rate, C, always enters in this at the same kt-y value because there is either a full contribution of C directly (WB Fit) or two independent contributions of C/2 (subtraction methods). (The analysis can be generalized to determine the optimum ratio for subdividing the total volume. It is close to 1:1.)

The following basic rates per kt-y are input:

$$N = 2315 = 0.388(4500 f_{SSM} + 1176 + 294) \quad (7)$$

$$C = 2241 \quad (8)$$

$$A = 234 \quad (9)$$

$$B = 0.388(78) = 30 \quad (10)$$

These are, respectively, the NC, CC, Acrylic, and membrane rates (median-plane split) at the reference activities. The quantity f_{SSM} is the fraction of the SSM rate in neutral currents. The factor 0.388, the fraction of neutron capture events falling above the 60-hit threshold, is derived from FB via eq.(7). The variance in the total (NC + internal) neutron rate is then given by

$$\sigma_N^2 = \frac{Cf_1 + Nf_2 + Af_3 + Bf_4}{(1 - \sum_{i,i\neq N} \rho_{iN}^2)}. \tag{11}$$

The factors f_i represent geometry and/or time multipliers for the basic signals in each method. They are generally self-explanatory, except that the value for f_3 for the bladder is derived from the fraction of the Gaussian of Acrylic background that falls inside the bladder (FB parameters). The following table summarizes the relevant quantities for each method:

	f_1	f_2	f_3	f_4	ρ_{NA}	ρ_{NB}	ρ_{NC}
WB Fit	1.0	1.0	1.0	0.0	-0.27	0.0	-0.71
WB Time-Seq.	1.0	0.5	0.5	0.0	-0.27	0.0	0.0
Median Split	1.0	0.6	0.5	1.0	-0.27	-0.27	0.0
Bladder	1.0	0.5	0.14	2.0	-0.27	-0.27	0.0

Since each method must deal with the same internal background, and methods for determining it are independent of which method is used, it is most useful to evaluate and compare σ_N without subtracting the internal neutron background. However, it must be remembered that the 20% error in determining the internal background makes a contribution that all but swamps statistical errors, except when background levels from acrylic and membrane material are enormous.

Figures 8 and 9 show σ_N/N for, respectively, acrylic and membrane radioactivities up to 100 times larger than the reference designs. The deleterious effect of NC-CC correlation can be seen very clearly in the WB-Fit method. The other 3 methods have comparable statistical power. Even very serious acrylic and membrane activity underestimates do not damage the experiment fatally.

From these results, we conclude that:

1. All Čerenkov methods except NC-CC fitting are robust and of comparable statistical power.

2. While the bladder approach is marginally the best in raw statistical accuracy, the engineering advantages for construction, deployment, calibration, and probably cost, favor the median-plane split, which should be selected.

9 Non-Čerenkov Options

Discrete devices are placed in the heavy water, and neutrons that have thermalized and captured in the devices give a distinctive signal that cannot (or should not) be confused with CC events. Such methods have the following advantages over the Čerenkov options:

1. Neutrons are detected event-by-event in real time.

2. The CC and NC signals are not backgrounds to each other. If the two were equal, and if there were no other backgrounds, the statistical uncertainties on both would be halved.

3. For transient events such as a supernova, each event can be assigned a time accurate to a few milliseconds. Subtraction methods only permit extraction of the average time evolution of the signals.

4. Relatively straightforward access to the entire volume for calibrations.

5. No substances need to be dissolved in the heavy water.

Against these must be weighed the disadvantages:

1. Detectors are more complex and more difficult to install.

2. Purity requirements are stringent.

3. Direct radon-assay techniques are inapplicable for measuring the backgrounds of detector construction materials.

4. There is some scattering and absorption of light from CC events.

As has been discussed by Hargrove and Paterson[7], the choice of neutron capture target nucleus is in practice confined to 3 nuclei, ^{3}He, ^{6}Li, and ^{10}B, because only these have large cross sections and charged-particle decay products. Compact detectors with fully contained events are possible. Decay products are detected in a gas to avoid the pulse-height defects associated with the heavier charged particles in the case of scintillators, or to make use of gas proportional counting.

9.1 ^{3}He Proportional Counters

For the reference design [2, 4] the calculated neutron-capture probability is 42%. The reaction is:

$$^3\mathrm{He} + \mathrm{n} \rightarrow \mathrm{T} + \mathrm{p} + 0.764\ \mathrm{MeV}.$$

For pure helium, in 31% of captures, either the triton or the proton strikes the wall before the end of its range (see Fig. 10). The wall effect drops with the addition of Xe, owing to the higher stopping power of the heavier gas. The range R (length units) in the mixture is

$$\frac{1}{R} = \frac{P_{Xe}}{R_{Xe}} + \frac{P_{He}}{R_{He}}, \tag{12}$$

where the quantities P_x are the proportions by pressure of the component gases. With 10% Xe, the wall effect is 21%; thus 80% of the events fall in the main peak. Wall effect events can also be used since the spectrum is known, but the signal-to-noise ratio is worse in that part of the spectrum. To be conservative, we assume an effective neutron efficiency of 0.42 x 0.80 = 34%.

Backgrounds have the following origins:

1. U and Th in construction materials cause photodisintegration of deuterium, producing a total of 140 neutrons per kt-yr in the heavy water.

	Th	U	Total
Acrylic	98	15	113
Glass	18	1	19
Copper	6	1	7

2. U and Th in the inner surfaces of the counters produce alpha particles that range out in the gas. This continuous background amounts to 930 counts per year underlying a peak of 10% resolution FWHM, if copper contains U and Th at the limits given.

3. Electrons can lose sufficient energy in the gas to reach 764 keV only through extensive multiple scattering. Monte Carlo calculations indicate that less than 10^{-5} of electrons having at least that much energy will scatter sufficiently. Little is known about total electron rates in the range 0.7 to 2 MeV, but contributions from the Th and U chains are negligible. Potassium must be kept to less than 10^{-4} total K by weight in the heavy water and acrylic.

4. Proportional counters are prone to electrical transients of various origins [11]. It is assumed that this effect can be reduced to an insignificant level through careful construction practice, electrical shielding, and pulse-shape analysis.

9.2 ^{3}He Scintillators

Mixtures of He with Xe are scintillators, with most of the light emission in the UV. The visible component can be enhanced by wavelength shifters. Preliminary measurements indicate that He-Xe by itself would give about 35 hits, and is stable over the long term. We assume that a wavelength shifter will be found that will increase this to about 100 hits without compromising the stability. Failing that, this method is not viable. The resolution is determined entirely by photoelectron statistics, and is 24% FWHM at 100 hits. The neutron efficiency and wall effects are the same as with proportional counters, but the slightly worse resolution means that about 82% of the signal is in the peak.

Backgrounds have the following origins:

1. U and Th in construction materials cause photodisintegration of deuterium, producing a total of 415 neutrons per kt-yr in the heavy water.

	Th	U	Total
Silica	400	15	415

2. U and Th in the inner surfaces of the counters produce alpha particles that range out in the gas. This continuous background amounts to 2300 counts per year underlying a peak of 24% resolution FWHM, if silica contains U and Th at the limits given.

3. As with proportional counters, electron backgrounds are not expected to contribute.

9.3 ^{6}Li Proportional Counters

In this design, an update of an earlier one [3], 10-μm thick Li foils are placed in Xe counters. The reaction is

$$^6\text{Li} + \text{n} \rightarrow \text{T} + \alpha + 4.78 \text{ MeV}.$$

The recoiling α and triton are detected on opposite sides of the foil. The major advantage of this scheme is that α backgrounds from the U and Th decay chains are completely suppressed. Because the decay products must emerge from the Li foil and enter the gas, it becomes difficult to place enough Li in the detectors to be highly neutron efficient. The calculated sensitivity is 0.25 x 0.95 x 0.70 x 0.86 = 14%, where the factors are the neutron capture probability in ^{6}Li, the isotopic enrichment, the escape probability from the foil (Fig. 11), and a correction for neutron capture in Xe, respectively.

Only the proportional-counter realization of this approach is considered here. The use of scintillation light directed to opposite sides of the PMT array seems likely to create a difficult-to-interpret background to CC light for singles events.

Backgrounds have the following origins:

1. U and Th in construction materials cause photodisintegration of deuterium, producing a total of 266 neutrons per kt-yr in the heavy water. We lack information on the purities of any materials except acrylic.

	Th	U	Total
Acrylic	231	35	266
Other	?	?	?

2. Alpha activities make no contribution directly to the background.

3. Cascades in which an alpha or a beta is followed by a conversion electron can produce a coincidence in the energy band accepted. A sizeable fraction of 500-keV electrons stop in 1 cm of 10-atm Xe. Estimating this effect is quite difficult.

4. Electrons transiting a Li foil can deposit energy on both sides of the foil and produce a coincidence. Again, this background has not been estimated.

5. Proportional counters are prone to electrical transients. The coincidence requirement may help eliminate many of these spurious pulses.

9.4 Non-Čerenkov Methods Compared

The NC, internal, and acrylic neutron rates are the same as used for comparing the Čerenkov methods. However, we will not consider the effects of unexpectedly high acrylic radioactivity, because the treatment of the data as a function of radius to unfold acrylic radioactivity will be qualitatively the same in both approaches. One difference will arise from the reduced neutron absorption of the discrete detectors relative to NaCl. The 1/e distance for neutron transport from the acrylic is approximately 37 cm for NaCl and 48 cm for ^{3}He detectors. On the other hand, the probability that acrylic-generated neutrons will escape into the light water is higher, and there is no additional range spread caused by the propagation of 8.6-MeV gammas. The effect of these on extracting the NC and acrylic signals by the fitting approach of FB is likely to be small.

The expected signals and backgrounds for the 3 schemes considered are summarized below for the SSM (5000 neutrons per kt-y plus 1176 internal background and 234 acrylic background).

	Efficiency	n Bkg.	Other Bkg.	σ_N/N	σ_n/n
^{3}He PC	34%	140	930	2.5%	7.0%
^{3}He Scint.	34%	415	2300	2.9%	8.3%
^{6}Li PC	14%	266	0?	3.3%	8.0%

Statistically, there is little to choose between the methods, either in precision on total neutrons, or in final precision once the photodisintegration backgrounds have been determined to 20%.

Interference with the Čerenkov light from CC events in the heavy water has been estimated for the ^{3}He PC option by Skensved [13]. Approximately 20% of the CC photons are absorbed or scattered, and the threshold wall moves up 0.5 MeV (Fig. 12, 13). Although the ^{6}Li option has not been specifically calculated, the Li counter array has an effective area about 2.4 times higher than the ^{3}He PC array, and the effects scale roughly as that factor. If that scaling is correct, the ^{6}Li design would interfere very seriously with CC events. The ^{3}He scintillators are necessarily transparent, and with suitably shaped containers would offer less interference than the other non-Čerenkov schemes.

Because the full 1000-tonne D_2O mass is continuously utilized for CC measurement, and because there is no significant neutron-capture signal to act as a background, the statistical accuracy in the CC signal is improved almost a factor of 2 to 2% in comparison with the Čerenkov methods of NC detection. Statistical accuracy is particularly important for the CC events, because of the need to bin the data to search for MSW distortions, and the need to search for time dependence in the CC signal.

The Li-foil method has the advantage of strongly rejecting direct α backgrounds, the major background for ^{3}He detectors. Those backgrounds, however, have a relatively benign effect on the overall statistical accuracy. The low efficiency, interference with CC light, and complex construction of Li-foil detectors lead us to recommend that only gaseous systems should be pursued. If a decision on which is the most suitable gaseous system is forced now, it would be the proportional counter, because the scintillator technology has not been demonstrated. Absent a compelling reason to force the decision, some further R&D on the scintillator option is appropriate.

10 Recommendations

We summarize the recommendations of this report as follows:

1. *At the time SNO is commissioned, there should be at least 2 and not more than 3 neutral-current detection methods in hand.*
2. *The White Book option should remain the default pending R&D and engineering design on other methods. The default status should be re-*

evaluated as the project approaches completion.

3. *The White Book option should be supplemented by the capability for addition and removal of salt underground on a time scale less than a month.*

4. *One of the most important research objectives for the Collaboration is development of precise methods for determining the photodisintegration background.*

5. *Studies of wavelength-shifter additives should be discontinued.*

6. *Studies of scintillation additives should be justified on the basis of physics unrelated to NC detection, and engineering feasibility.*

7. *Engineering design for a median-plane split vessel should be initiated.*

8. *Studies of internal bladder options should be discontinued.*

9. *Engineering for the installation of ^{3}He detectors should be initiated.*

10. *R&D on He detectors should continue until a timely decision is made between scintillation and proportional counters, at which point the disfavored option should be dropped.*

11. *Studies of Li-foil counters should be discontinued.*

References

[1] W. Frati and E. Beier, "Extraction of CC, NC, and ES Signals – II" SNO-STR-91-?

[2] T. J. Bowles et al., "Detection of Neutral Current Neutrino Interactions in the Sudbury Neutrino Observatory" LA-UR-90-546, SNO-STR-89-36.

[3] C.K. Hargrove, D. Kessler, and D. Paterson, "Design of a Solid-scintillator based Neutral Current Detector" , SNO-STR-90-105.

[4] T. J. Bowles et al., "Status Report – Neutral Current Detection" LA-UR-90-545, SNO-STR-90-?

[5] D. Wark, "Wavelength Shifter or Liquid Scintillator in SNO: First Pass", SNO-STR-91-?

[6] R. B. Schubank, "Bladder with Dissolved Substances for NC", SNO-STR-91-?

[7] C. K. Hargrove and D. J. Paterson, "Solar Neutrino Neutral Current Detection Methods in the Sudbury Neutrino Observatory", SNO-STR-90-104

[8] J. N. Bahcall, K. Kubodera, and S. Nozawa, Phys. Rev. D 38, 1030 (1988).

[9] S. Ying, W. C. Haxton, and E. M. Henley, Phys. Rev. D 40, 3211 (1989).

[10] Ali et al. Phys. Rev. D 12, 3672 (1975).

[11] R. I. Ewing et al., IEEE Trans. Nucl. Sci. 37, 1165 (1990).

[12] R. G. H. Robertson, "Beads - an Option for Neutral Current Detection in SNO?" SNO-STR-90-99

[13] P. Skensved and B. C. Robertson, "Extraction of Data in SNO for various MSW Scenarios", SNO-STR-91-06, also SNO-STR-91-07.

Fig. 1. Spectra with and without NaCl in the full volume of heavy water for 6 months). Standard Solar Model flux.

Fig. 2. As Fig. 1, but SSM/3.

Fig. 3. Subtraction of spectra in Fig. 1. This is the net NC + internal neutron capture spectrum after one year's running.

Fig. 4. As Fig. 3, but SSM/3.

Fig. 5. Distribution of neutron captures for split vessel, one year at SSM.

Fig. 6. Distribution of neutron captures for split vessel for increased levels of acrylic radioactivity.

Fig. 7. Functional forms of radial dependences of major signals in SNO. From Frati and Beier [1].

Fig. 8. Statistical precisions (one standard deviation) in determination of total neutron rate (NC/SSM plus internal) for 4 Čerenkov options as the acrylic activity is increased up to 100 times.

Fig. 9. As Fig. 8, but for membrane activities increasing up to 100 times.

Fig. 10. Monte Carlo simulations of neutron-capture (top) and alpha background spectra from ^{3}He proportional counters. The wall effect is apparent in the upper plot. Ref. [4].

Fig. 11. Escape probability for α-triton pairs from Li foils vs. thickness. Ref. [3]

Fig. 12. Čerenkov spectra for major signals. Ref. [13].

Fig. 13. As Fig. 12, but with ^{3}He proportional counters installed.

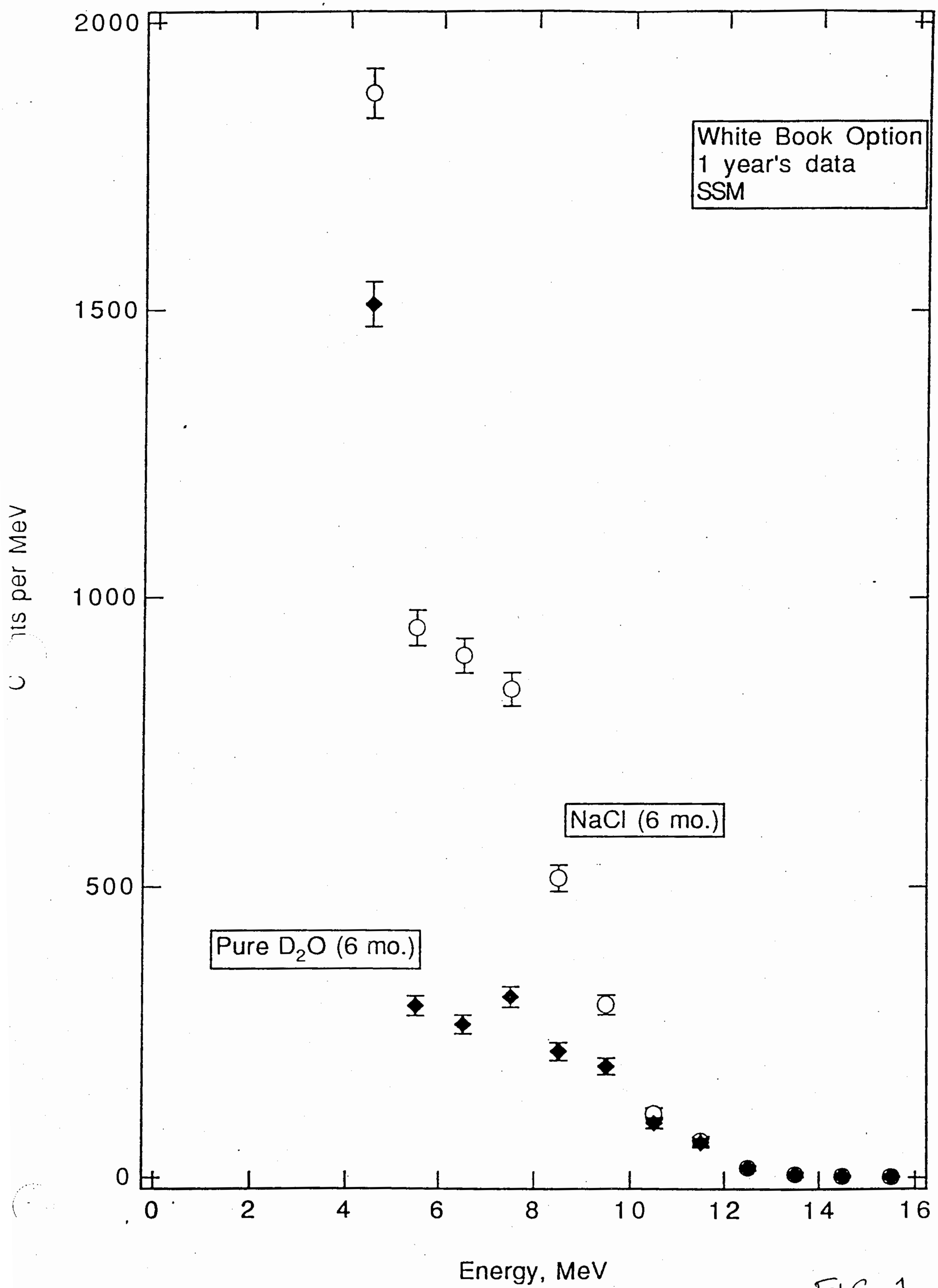

White Book Option
1 year's data
SSM
NaCl (6 mo.)
Pure D_2O (6 mo.)
Counts per MeV
Energy, MeV
0
500
1000
1500
2000
0
2
4
6
8
10
12
14
16

FIG. 1

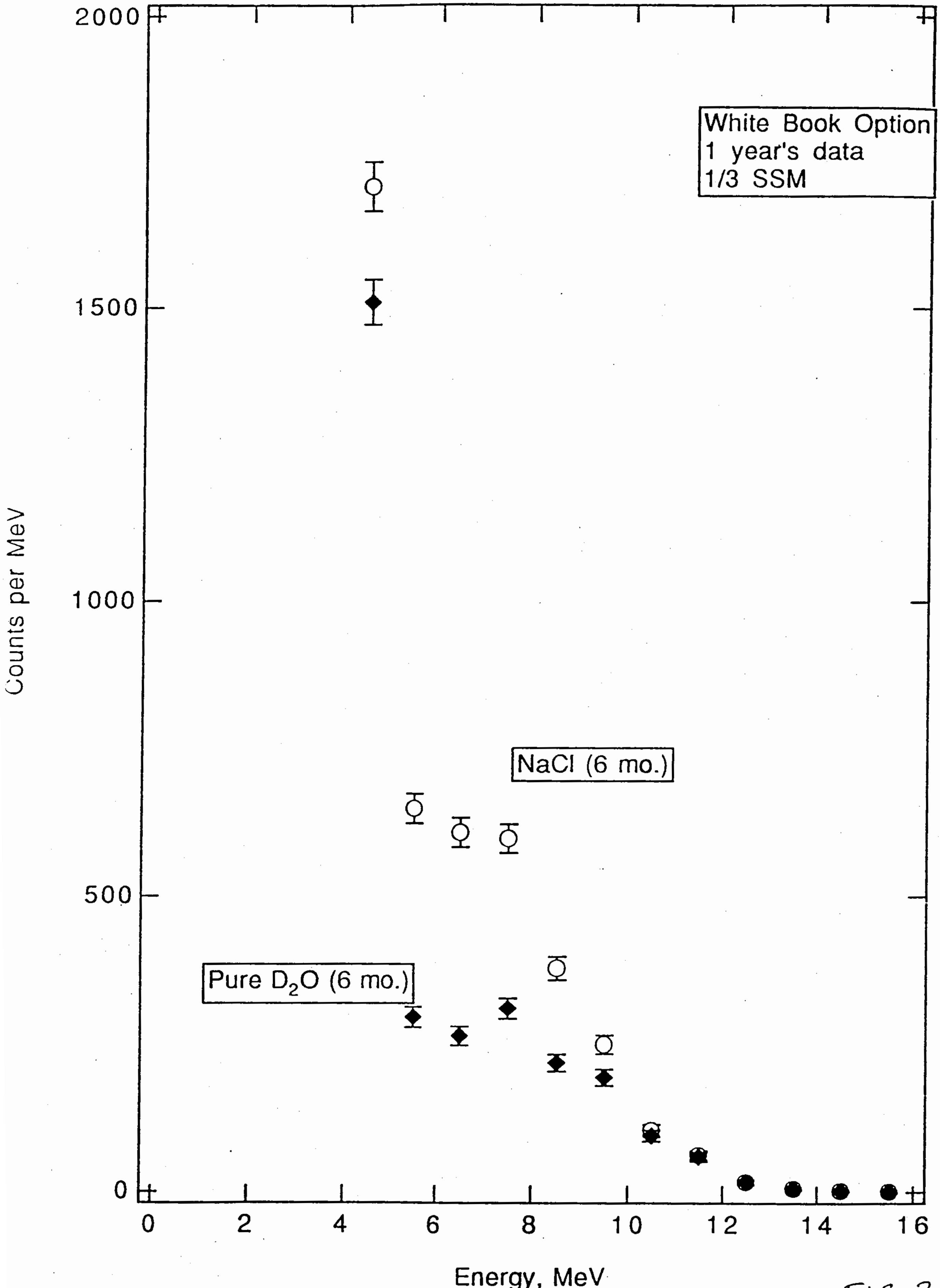
White Book Option
1 year's data
1/3 SSM
NaCl (6 mo.)
Pure D_2O (6 mo.)
Counts per MeV
2000
1500
1000
500
0
0
2
4
6
8
10
12
14
16
Energy, MeV

FIG. 2

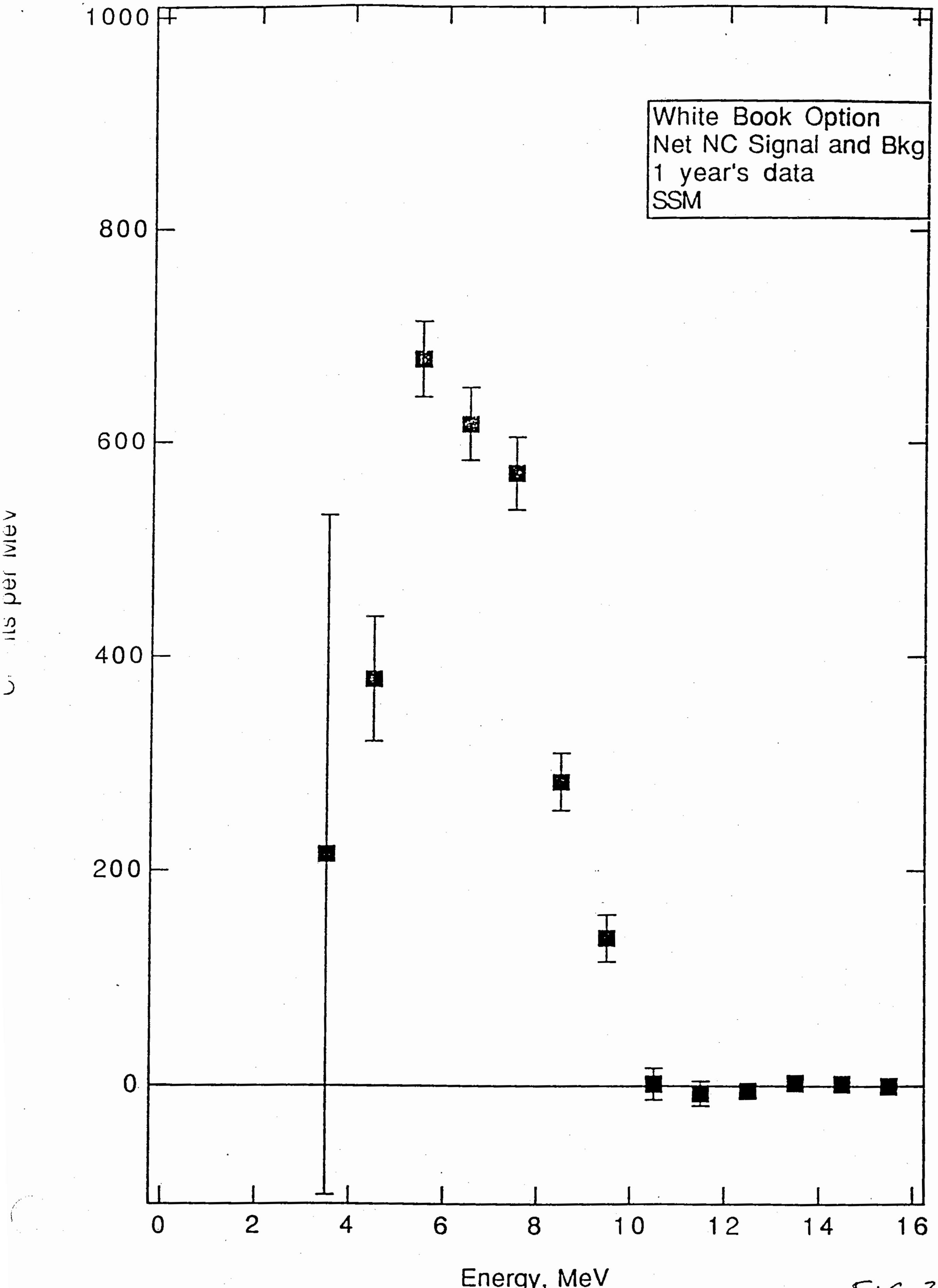
White Book Option
Net NC Signal and Bkg
1 year's data
SSM
1000
800
600
400
200
0
0
2
4
6
8
10
12
14
16
Energy, MeV

FIG. 3

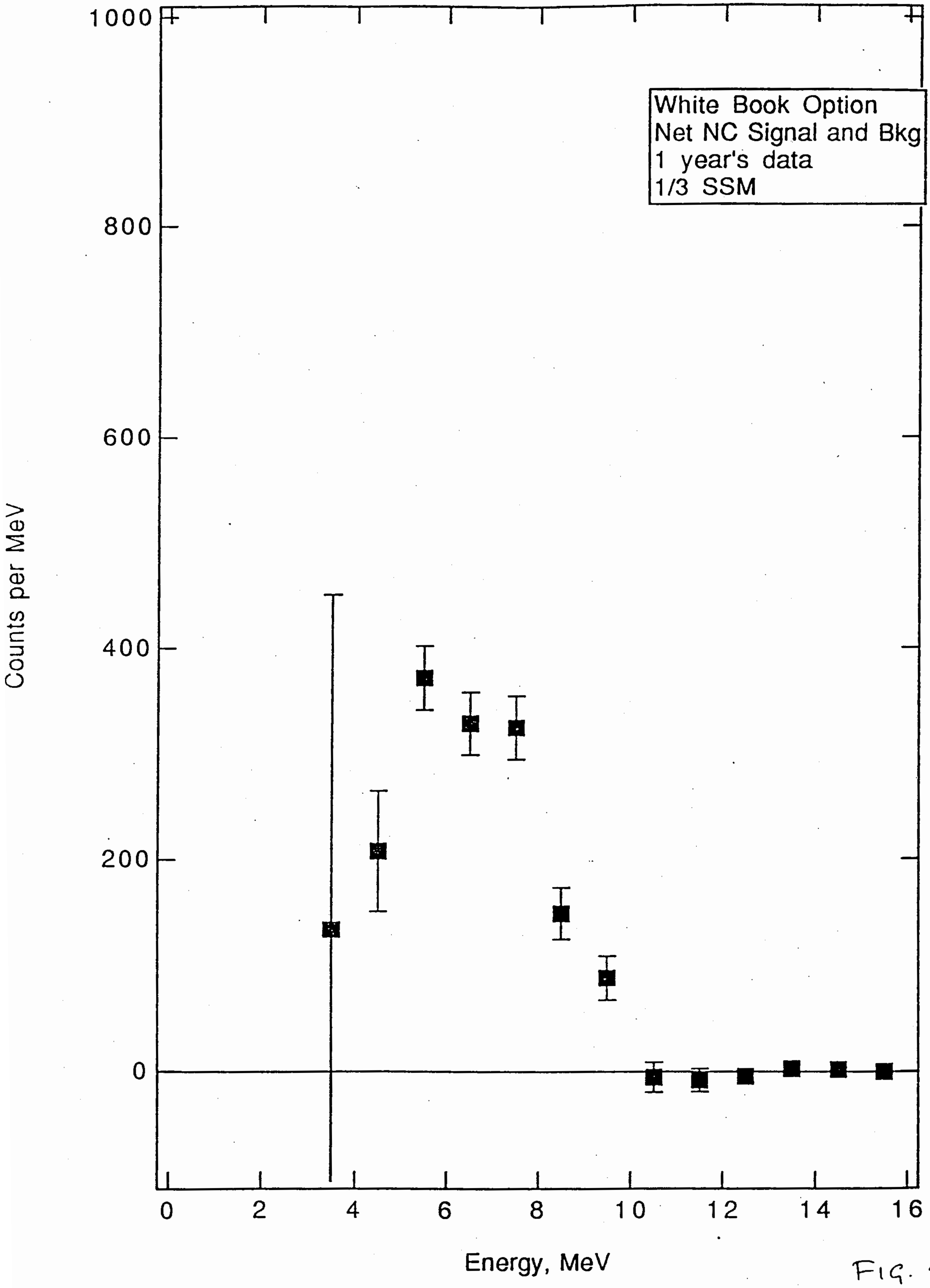
White Book Option
Net NC Signal and Bkg
1 year's data
1/3 SSM
Counts per MeV
Energy, MeV
1000
800
600
400
200
0
0
2
4
6
8
10
12
14
16

FIG. 4

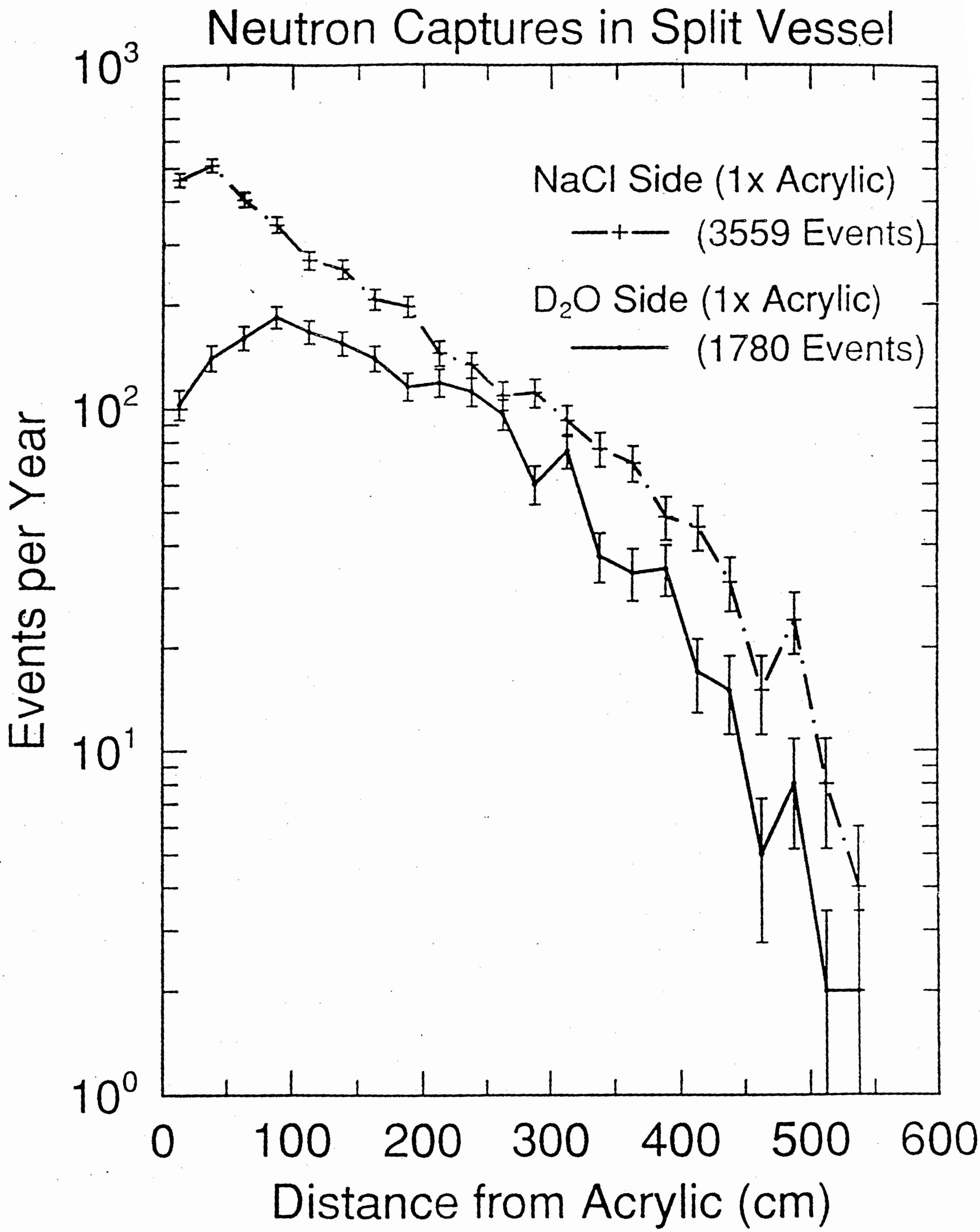
Neutron Captures in Split Vessel
10^3
10^2
10^1
10^0
Events per Year
NaCl Side (1x Acrylic)
(3559 Events)
D_2O Side (1x Acrylic)
(1780 Events)
0
100
200
300
400
500
600
Distance from Acrylic (cm)

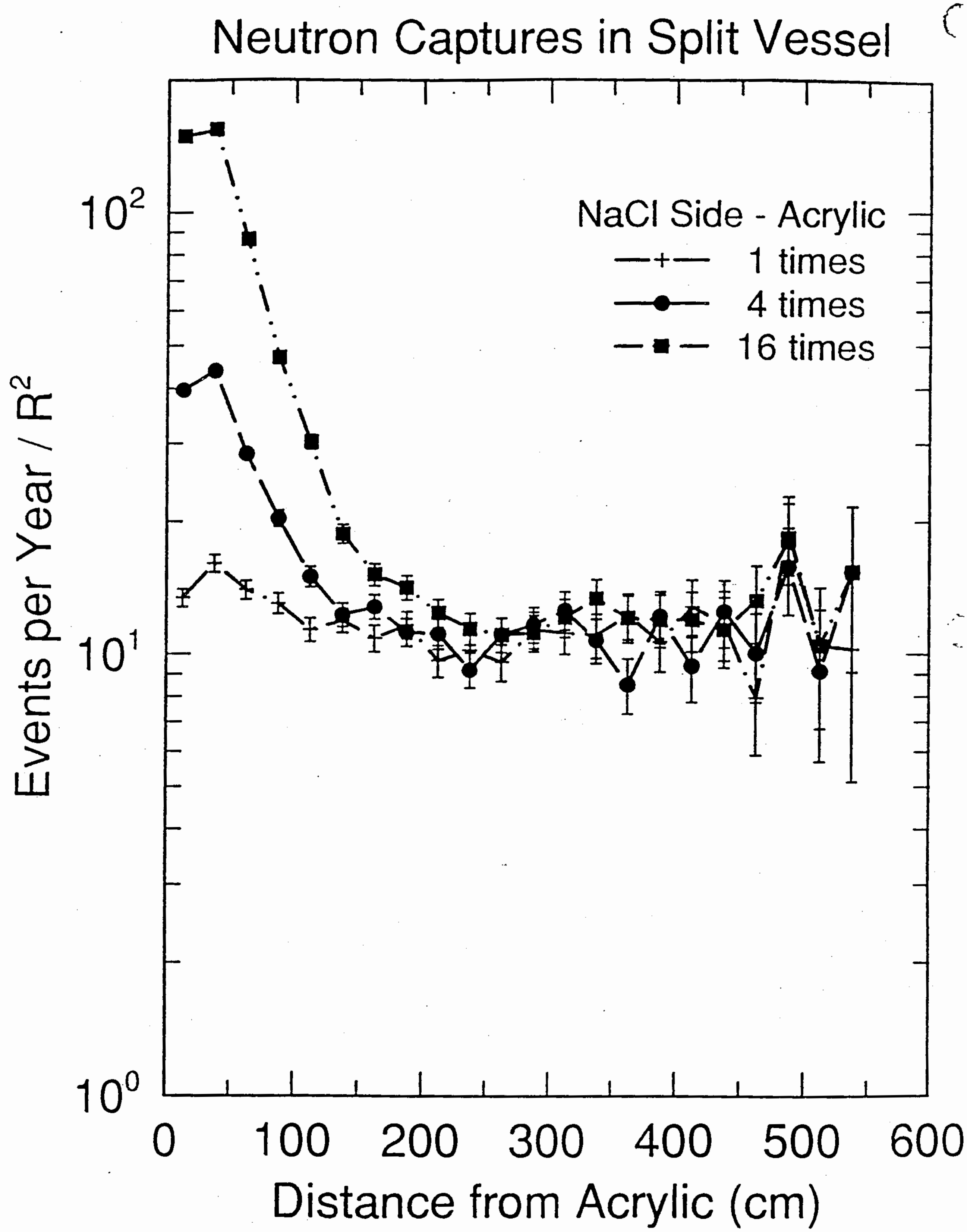

Neutron Captures in Split Vessel
NaCl Side - Acrylic
1 times
4 times
16 times
Events per Year / R^2
10^2
10^1
10^0
0
100
200
300
400
500
600
Distance from Acrylic (cm)

FIG. 6

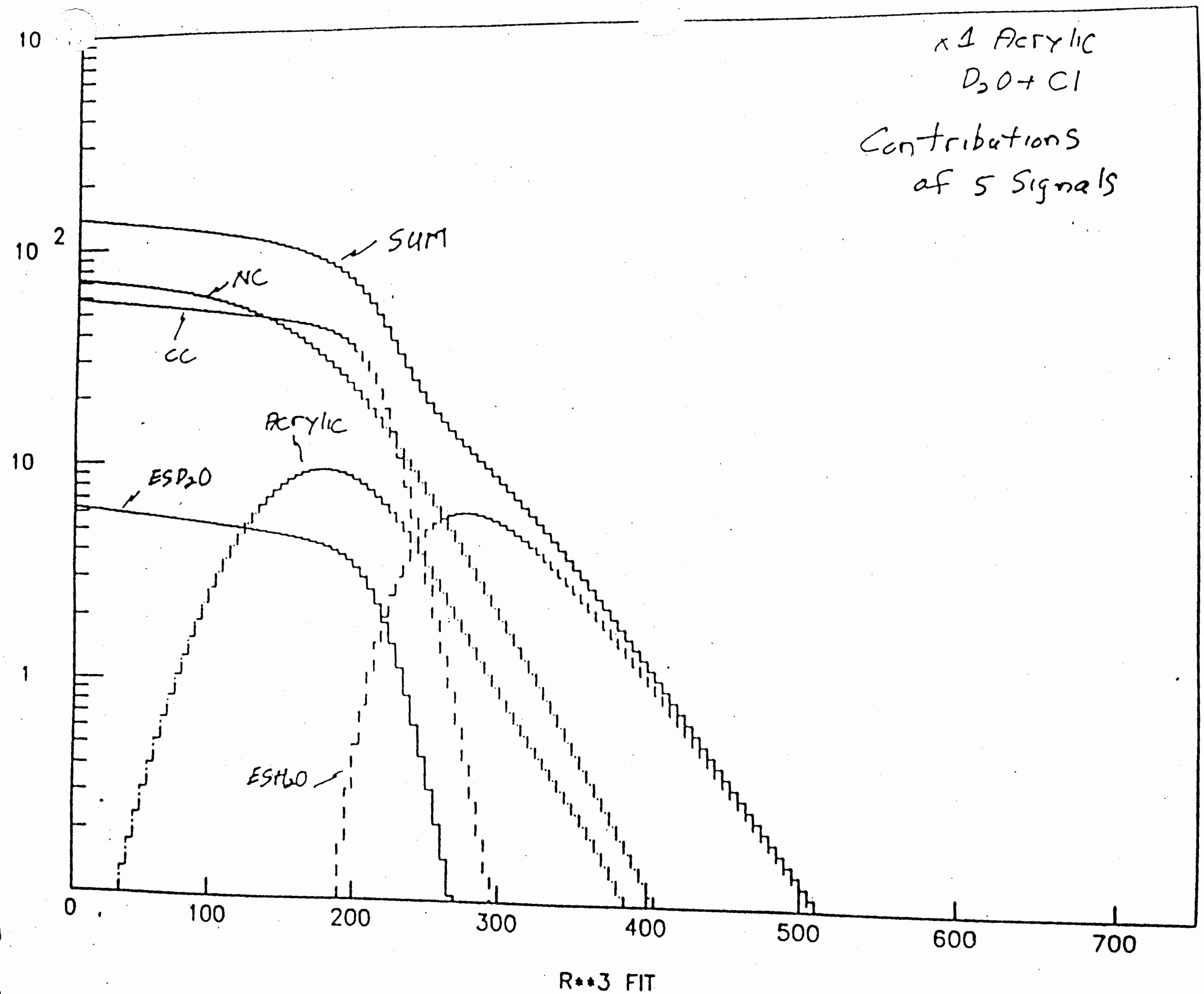

Fig 7d

Fig. 7

7C

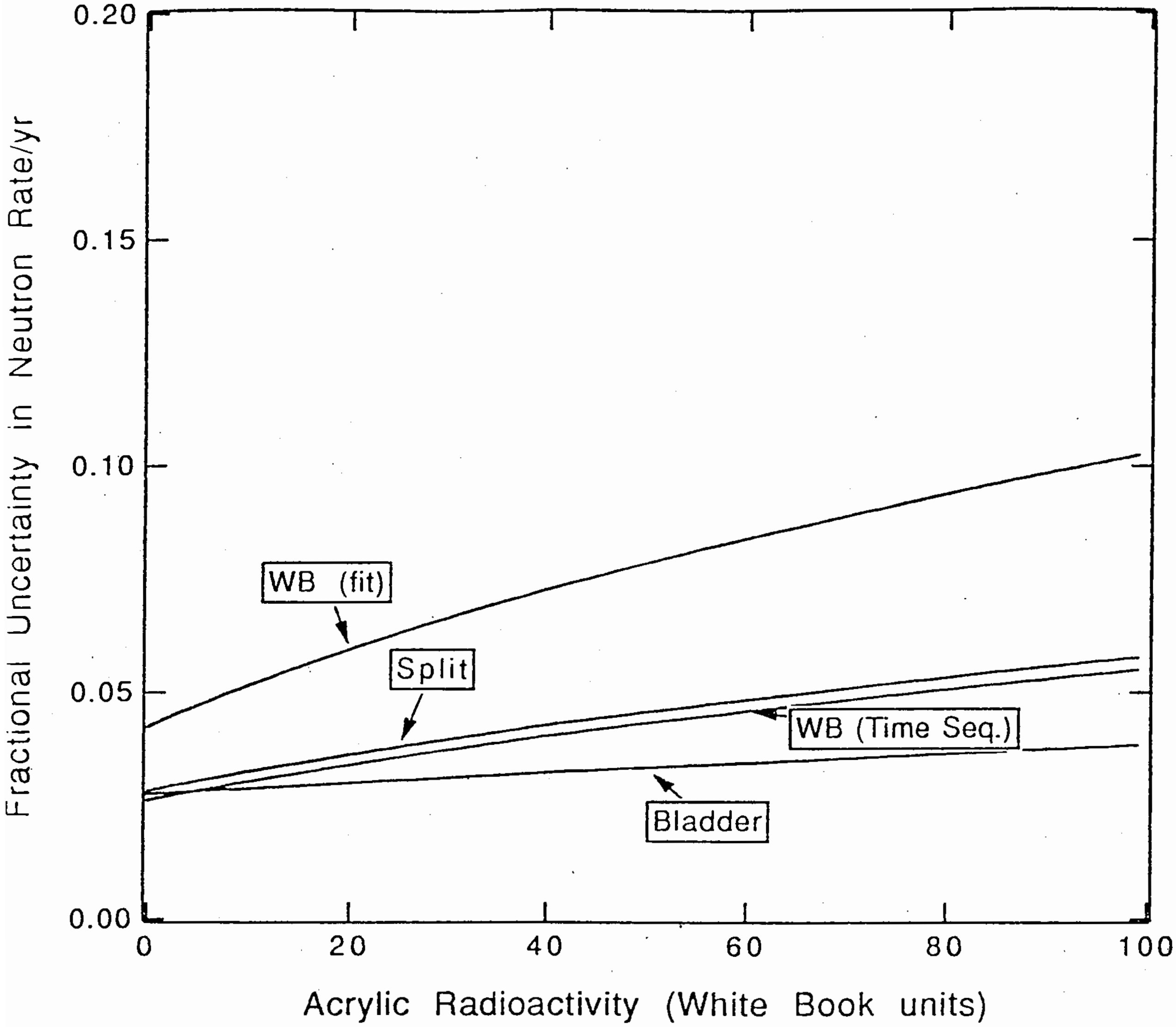
0.20
0.15
0.10
0.05
0.00
Fractional Uncertainty in Neutron Rate/yr
WB (fit)
Split
WB (Time Seq.)
Bladder
0
20
40
60
80
100
Acrylic Radioactivity (White Book units)

FIG. 8

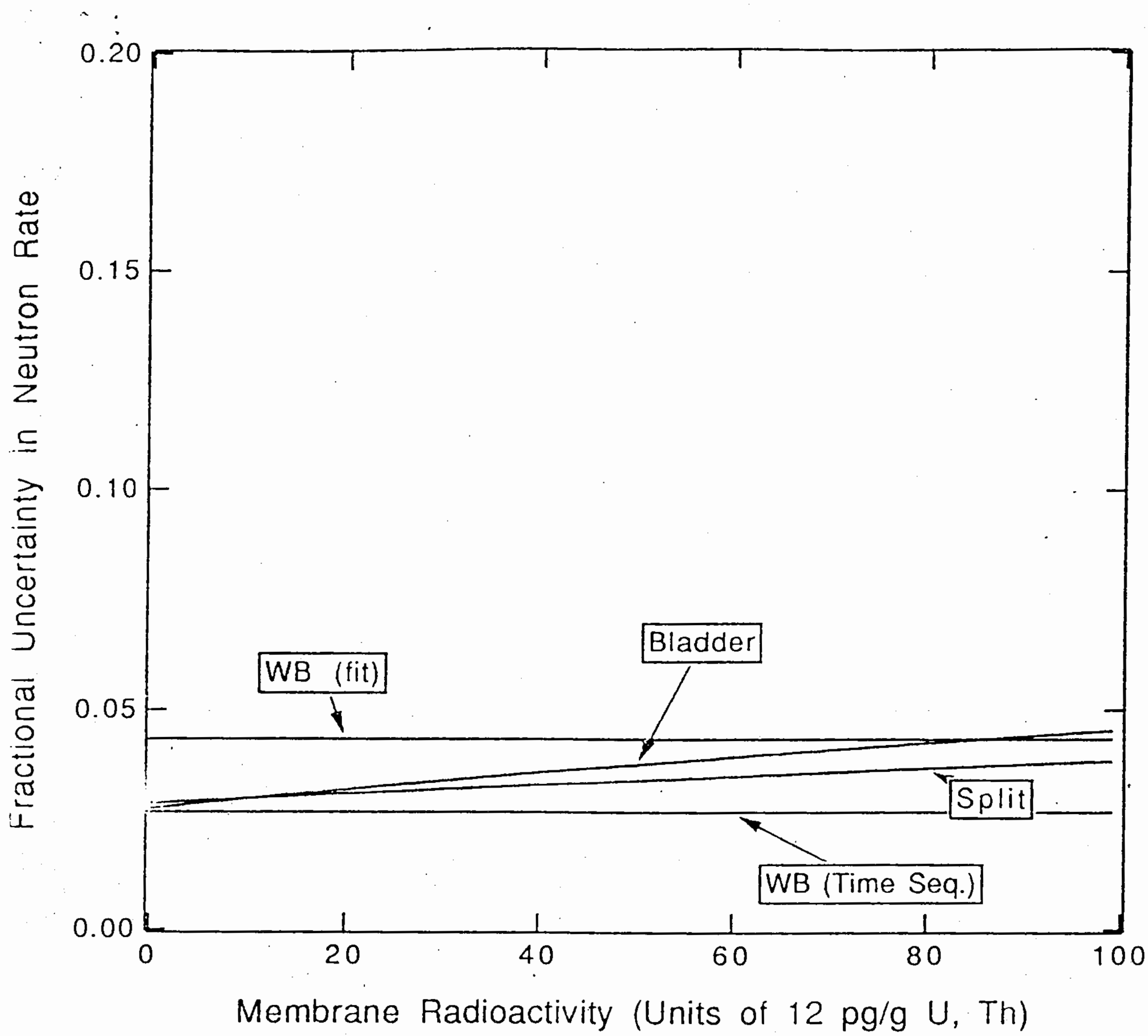
0.20
0.15
0.10
0.05
0.00
Fractional Uncertainty in Neutron Rate
WB (fit)
Bladder
Split
WB (Time Seq.)
0
20
40
60
80
100
Membrane Radioactivity (Units of 12 pg/g U, Th)

FIG. 9

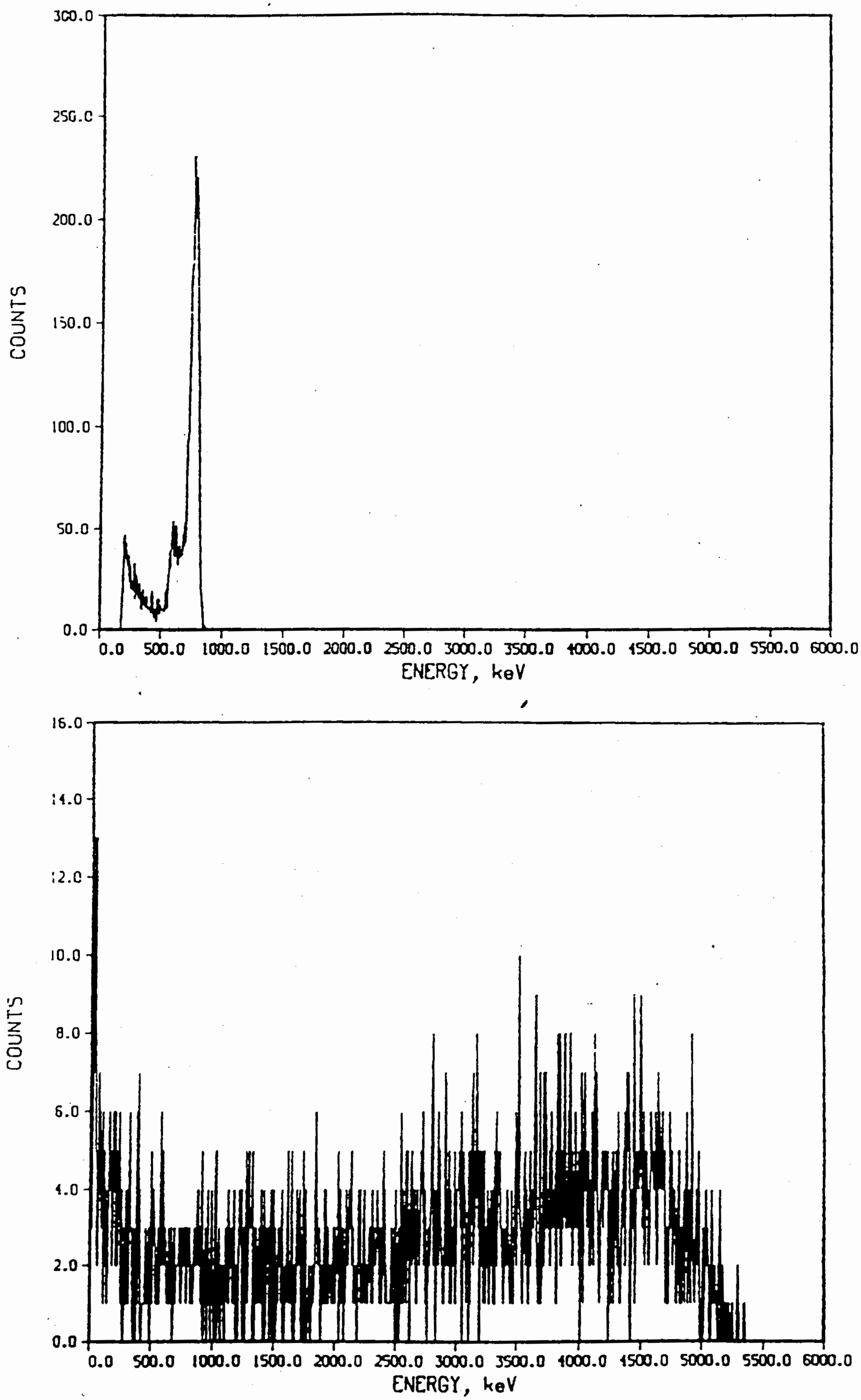

300.0
250.0
200.0
150.0
100.0
50.0
0.0
COUNTS
0.0 500.0 1000.0 1500.0 2000.0 2500.0 3000.0 3500.0 4000.0 4500.0 5000.0 5500.0 6000.0
ENERGY, keV
16.0
14.0
12.0
10.0
8.0
6.0
4.0
2.0
0.0
COUNTS
0.0 500.0 1000.0 1500.0 2000.0 2500.0 3000.0 3500.0 4000.0 4500.0 5000.0 5500.0 6000.0
ENERGY, keV

FIG. 10

Detection Efficiency vs. Li layer thickness.

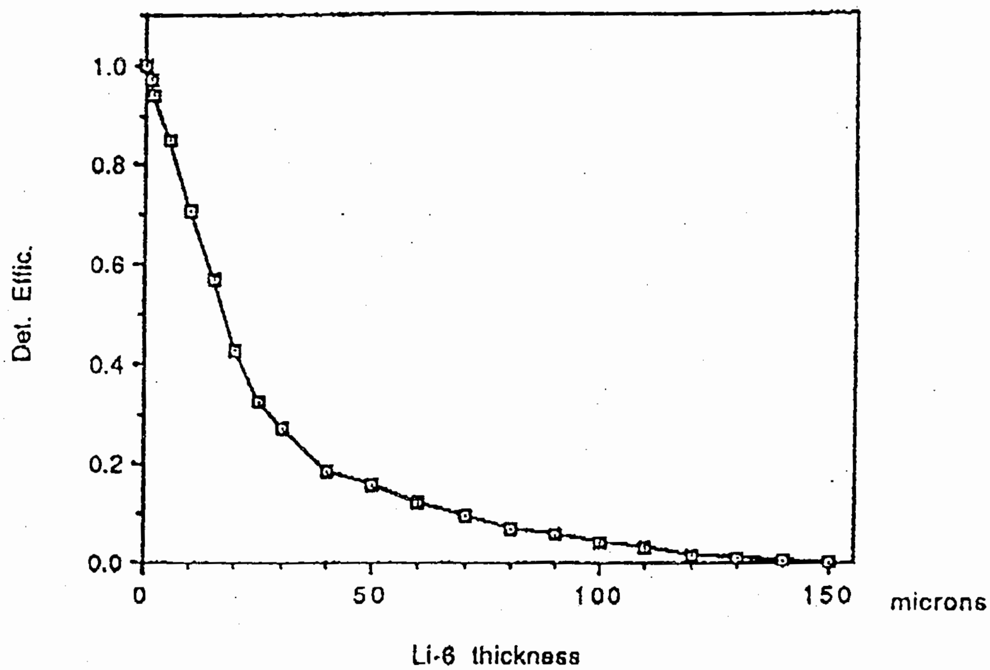

D.K.

Figure 1.

FIG. 11

Fig. 1

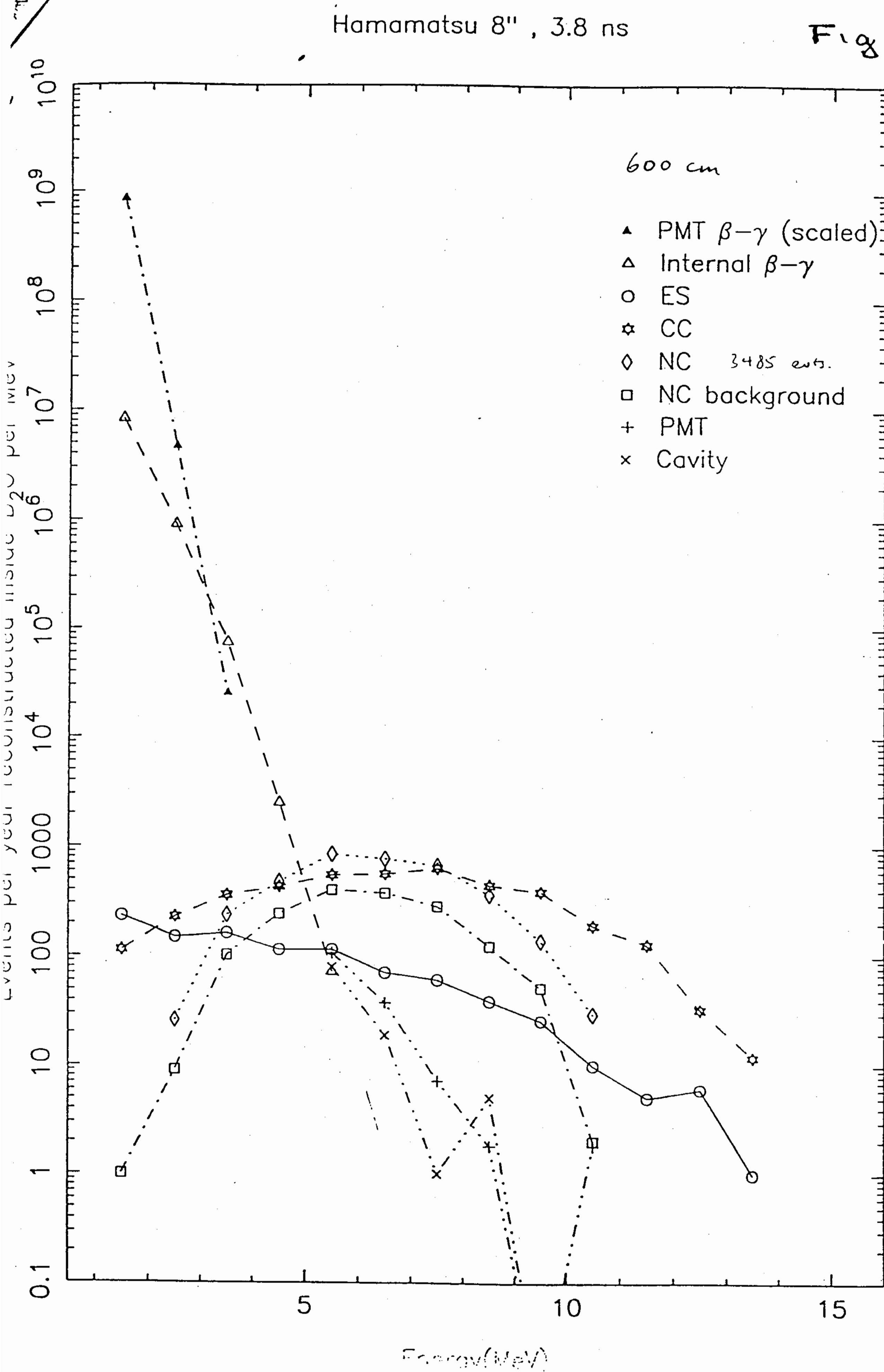
Hamamatsu 8" , 3.8 ns
600 cm
PMT β−γ (scaled)
Internal β−γ
ES
CC
NC 3485 evts.
NC background
PMT
Cavity
Events per year reconstructed inside D2O per MeV
Energy(MeV)
0.1
1
10
100
1000
10^4
10^5
10^6
10^7
10^8
10^9
10^10
5
10
15

FIG. 12

Hamamatsu 8" , 3.8 ns with ^{3}He tubes

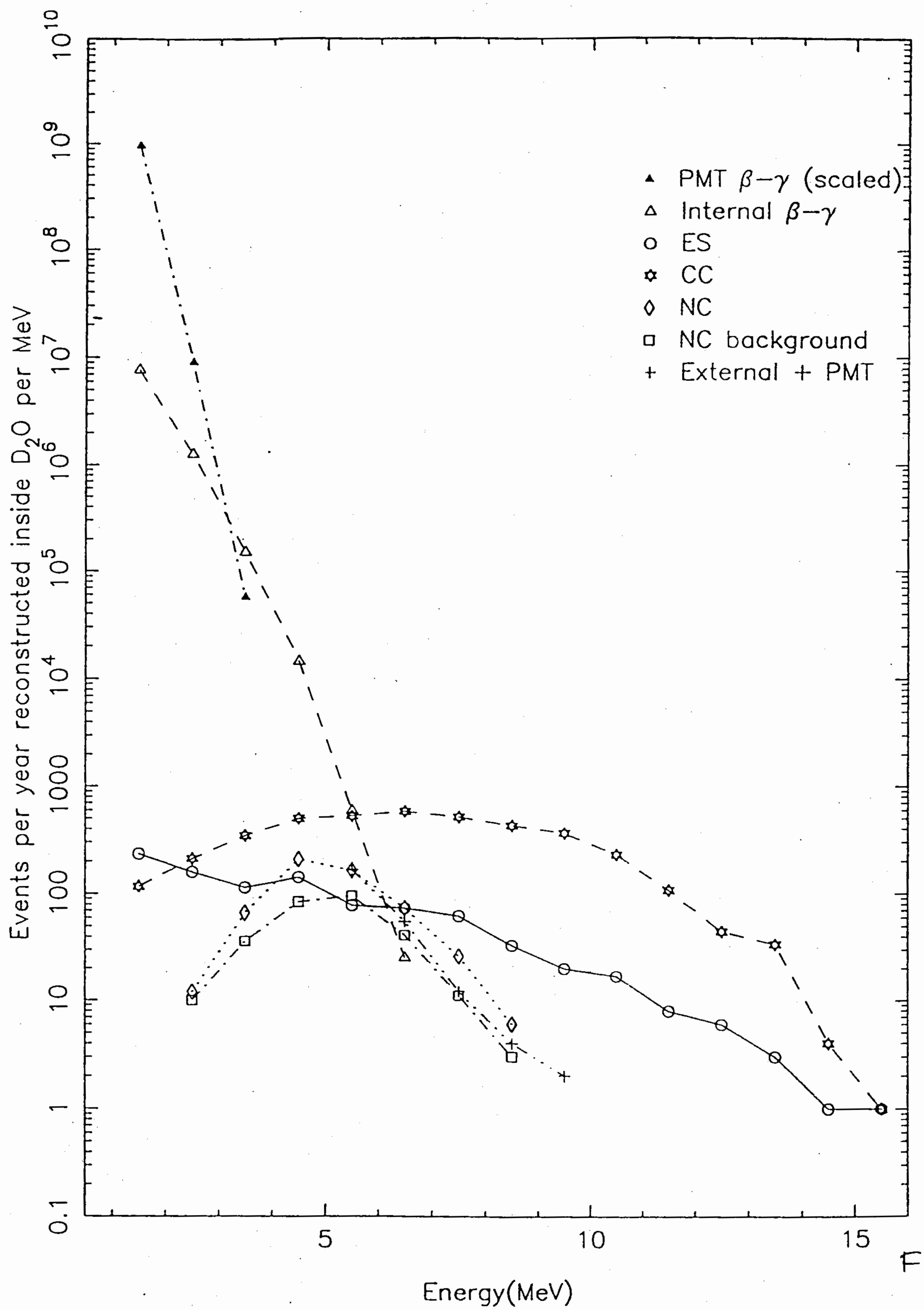

FIG. 13